

1 **The TFIIH components p44/p62 act as a damage sensor during** 2 **nucleotide excision repair**

3 Barnett JT¹, Kuper J², Koelmel W², Kisker C² and Kad NM^{1,*}

4 ¹ School of Biological Sciences, University of Kent, Canterbury, CT2 7NH, United Kingdom.

5 ² Rudolf Virchow Center for Experimental Biomedicine, Institute for Structural Biology, University of
6 Würzburg, 97080 Würzburg, Germany.

7 * To whom correspondence may be addressed. Email: n.kad@kent.ac.uk

8
9 Keywords; DNA repair, NER, fluorescence imaging, single molecule

10

11 **Abstract**

12 Nucleotide excision repair (NER) protects the genome following exposure to
13 diverse types of DNA damage, including UV light and chemotherapeutics.
14 Mutations in human NER genes lead to diseases such as xeroderma
15 pigmentosum and Cockayne syndrome ¹. In eukaryotes, the major transcription
16 factor TFIIH is the central hub of NER. The core components of TFIIH include
17 the helicases XPB, XPD, and the five core ‘structural’ subunits ²⁻⁶. Two of these
18 core-TFIIH proteins, p44 and p62 remain relatively unstudied; although p44 is
19 known to regulate the helicase activity of XPD during NER ⁷⁻⁹. p62’s role is
20 thought to be structural ¹⁰; however, a recent cryo-EM structure ¹¹ shows p44,
21 p62, and XPD making contacts with each other, implying a more extensive role
22 in DNA repair beyond the structural integrity of TFIIH. Here, we show that p44
23 stimulates XPD’s ATPase, but upon encountering DNA damage further
24 stimulation is only observed when p62 is in the ternary complex. More
25 significantly, we show that the p44/p62 complex binds DNA independently of
26 XPD and diffuses along its backbone, indicating a novel DNA-binding entity in
27 TFIIH. These data support a role for p44/p62 in TFIIH’s mechanism of damage
28 detection. This revises our understanding of TFIIH and prompts more extensive
29 investigation of all of the core subunits, for an active role during both DNA
30 repair and transcription.

31 **Results and Discussion**

32

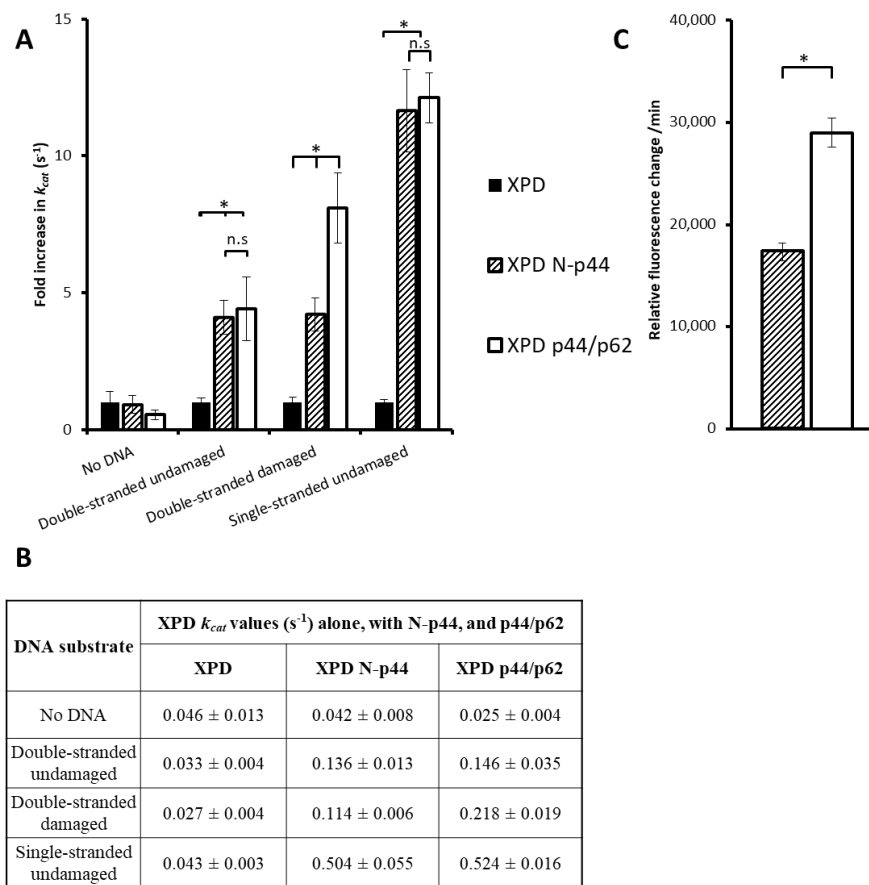
33 **XPD's ATPase is stimulated by p44/p62**

34 p44 contacts both p62 and XPD in TFIIH^{3,11,12}, and mutations in XPD that
35 disrupt p44 or p62 binding cause defects in NER and result in disease^{3,7,8,12}. To
36 investigate if p44/p62 was able to stimulate the ATPase of XPD, the turnover of
37 ATP in the presence of different DNA substrates was measured using an
38 NADH-coupled assay.

39 In the absence of p44 and p62, XPD's ATPase activity is slow even in the
40 presence of single-stranded DNA (0.043 s⁻¹). However, with a p44 fragment
41 (residues 1-285 (N-p44)) containing the von Willebrand domain, XPD's
42 ATPase was significantly stimulated in the presence of both double- and single-
43 stranded DNA⁸ (~0.03 s⁻¹ to 0.136 s⁻¹ and 0.504 s⁻¹ respectively $p < 0.05$
44 (**Figure 1**)). No further acceleration of the ATPase was observed with full
45 length p44 co-expressed in complex with p62 (p44/p62). However, remarkably,
46 when damage (a fluorescein moiety shown to proxy for damage¹³) was
47 introduced into a dsDNA substrate, p44/p62 accelerated XPD's ATPase two-
48 fold more than on undamaged DNA (**Figure 1A & B**). N-p44 alone could not
49 accelerate XPD's ATPase in the presence of damage, indicating the ternary
50 complex (p44/p62) is responsible for this further enhancement and thus may
51 play an important role in lesion detection. These results may explain why
52 truncations of the yeast p62 homologue (Tfb1) sensitize the organism to UV
53 irradiation¹⁴⁻¹⁶.

54 To further investigate the role of p44 and p62 in activating XPD we analyzed
55 XPD's helicase activity on an open fork substrate. Again, p44/p62 is seen to
56 play an active role by enhancing the helicase activity compared to N-p44 alone
57 (**Figure 1C**). Although no damage is present in the open fork substrate, p44/p62
58 significantly enhances XPD's ability to successfully unwind the DNA substrate

59 (two-fold more than XPD with N-p44), despite no change in ATPase activity
 60 (**Figure 1A**).



61 **Figure 1. Steady-state ATPase and helicase activity of XPD in the presence of**
 62 **various DNA substrates and core TFIID proteins.** A) The activity of XPD's
 63 ATPase is stimulated by both N-p44 (dashed) and p44/p62 (white) on various
 64 DNA substrates. Values for k_{cat} are given as a fold change from XPD alone
 65 (black). Errors are shown as S.E.M from 3 repeats. B) Table showing k_{cat} values
 66 ± S.E.M for XPD's ATPase. C) XPD's helicase activity is stimulated by N-p44
 67 (dashed) and p44/p62 (white) on an open fork substrate. XPD alone displays no
 68 helicase activity⁸. Errors are shown as S.E.M from 9 repeats. Statistical

69 *significance determined using a student's t-test where * = $p < 0.05$, n.s = not*
70 *statistically significant.*

71

72

73 **The p44/p62 complex directly binds DNA**

74 The role of p44/p62 in the recognition of damage presents the intriguing
75 possibility that this complex could interact with DNA independently from XPD.

76 To investigate this, we used a single molecule DNA tightrope assay ¹⁷ (**Figure**

77 **2**). Conjugation of a fluorescent quantum dot (QDot) to the poly-histidine

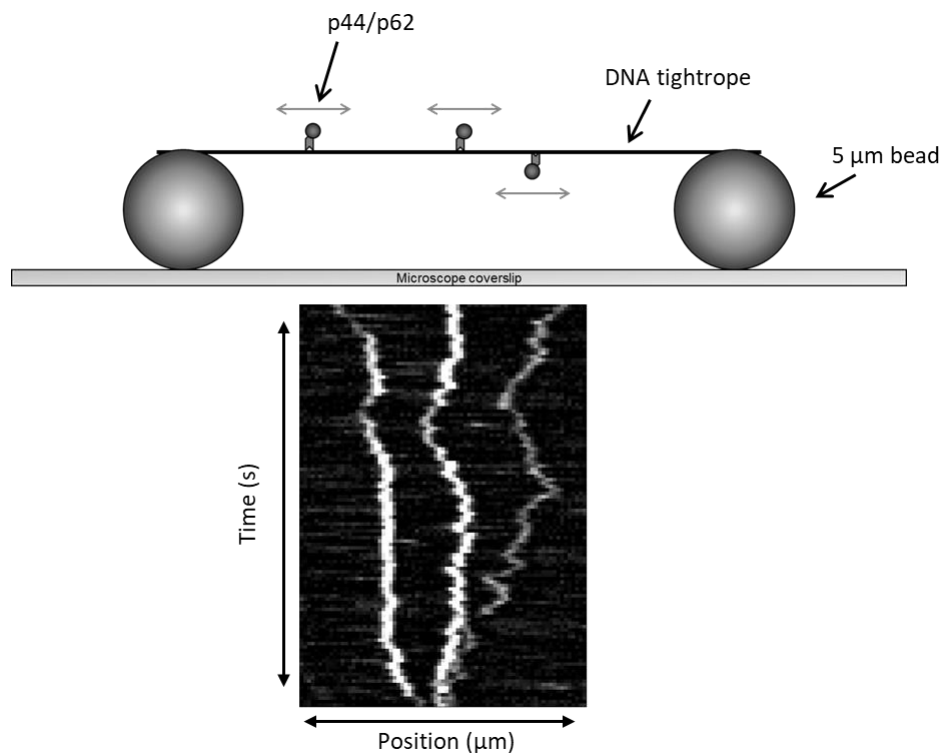
78 purification tag on the p44/p62 complex ¹⁸ was achieved using an anti-His IgG

79 antibody. Substantial binding of p44/p62 to dsDNA was observed, and of these

80 approximately 80% could diffuse (n = 599 total) providing the first direct

81 evidence that these TFIIH subunits are able to bind DNA independently of

82 XPD.



83 **Figure 2. Schematic of a tightrope and kymograph analysis.** DNA tightropes
84 are formed between beads adhered to a coverslip. QDot labelled proteins are
85 then observed binding to the DNA. A video can be transformed into a
86 kymograph by plotting position through time. Diffusing molecules appear as
87 movement in the X axis for a duration of frames (Y axis). The kymograph shown
88 in the lower panel indicates three diffusing p44/p62 molecules.

89
90 The p44/p62 complex displayed multiple types of behavior on DNA. Firstly, we
91 observed complexes randomly diffusing along the DNA, unable to pass one
92 another (**Figure 2**). Secondly while diffusing, pausing was seen, often at the
93 same location on the tightropes. This may indicate a visit to a damage site or a
94 specific sequence. Finally, fluorescence intensity fluctuations of the same
95 molecule over time suggest possible oligomerization. At elevated salt
96 concentrations (100 mM vs 10 mM KCl) fewer molecules bound to DNA, and
97 of these, a lower percentage diffused (55%, n = 58 total). We calculated the
98 diffusion constant using mean-squared displacement analysis¹⁷ and found no
99 significant change (p > 0.05) between salt conditions (10 mM KCl $0.067 \mu\text{m}^2/\text{s}$
100 ± 0.006 vs 100 mM KCl $0.042 \mu\text{m}^2/\text{s} \pm 0.010$), which suggests that p44/p62
101 molecules slide along the DNA helix¹⁹. Based on the estimated size of a
102 p44/p62 complex conjugated to a QDot, the diffusion constant appears limited
103 by rotation-coupled diffusion around the backbone of the DNA helix²⁰. This is
104 consistent with the inability for complexes to pass one another on the DNA.

105
106 In summary, we present the first mechanistic characterisation of the non-
107 helicase TFIIH subunits p44/p62. Complexes formed by these two proteins
108 were observed to bind and slide on dsDNA. Our bulk phase ATPase and
109 helicase data indicate that p44/p62 is involved in damage recognition. One
110 could speculate that p44/p62 actively enhances TFIIH activity towards scanning
111 the opened repair bubble to position TFIIH factors for subsequent excision.

112 Nonetheless, our results clearly show that the p44/p62 complex plays an active
113 and not just a structural role in the TFIID complex.

114

115

116 **Methods**

117 *Purification*

118

119 The genes encoding p44 and p62 were cloned from *C. thermophilum* cDNA.
120 p62 was cloned into the pETM-11 vector (EMBL) without a tag. p44 was
121 cloned into the pBADM-11 vector (EMBL) containing an N-terminal hexa-
122 Histidine tag followed by a TEV cleavage site. p62 and p44 were co-expressed
123 in *E. coli* BL21 CodonPlus (DE3) RIL cells (Agilent) and were co-purified via
124 immobilized metal affinity chromatography (Ni TED, Machery-Nagel),
125 followed by size exclusion chromatography (SEC), and anion exchange
126 chromatography (AEC). SEC was conducted with a HiLoad 16/600 Superdex
127 200 prep grade column (GE Healthcare) in 20 mM Hepes pH 7.5, 250 mM
128 NaCl, and 1 mM TCEP. AEC was conducted with a MonoQ 5/50 GL column
129 (GE Healthcare). The proteins were eluted via a salt gradient ranging from 50 to
130 1000 mM NaCl. AEC buffers were composed of 20 mM HEPES pH 7.5,
131 50/1000 mM NaCl, and 1 mM TCEP. The p62/p44 protein complex was
132 concentrated to approximately 20 mg/ml and flash frozen in liquid nitrogen for
133 storage.

134 XPD and N-p44 (1-285) from *C. thermophilum* were cloned as described
135 previously²¹. XPD was expressed as N-terminally His-tagged proteins in *E. coli*
136 ArcticExpress (DE3)-RIL cells (Agilent). Cells were grown in TB medium at
137 37°C until they reached an OD₆₀₀ of 0.6-0.8. Expression was started with the
138 addition of 0.05% L-arabinose and performed at 11°C for 20 h. p44 was
139 expressed as N-terminally His-tagged protein in *E. coli* BL21-CodonPlus
140 (DE3)-RIL cells (Stratagene). Cells were grown as described for ctXPD and

141 expression was started by adding 0.1 mM IPTG at 14°C for 18 h. XPD and p44
142 were purified to homogeneity by metal affinity chromatography (Ni-IDA,
143 Macherey&Nagel) as described previously ²¹ followed by size exclusion
144 chromatography (SEC) (20 mM HEPES pH 7.5, 200 mM NaCl) and an
145 additional anion exchange chromatography (AEC) step in the case of XPD.
146 AEC was performed using a MonoQ 5/50 GL column (GE Healthcare) with 20
147 mM HEPES pH 7.5, 50 mM NaCl, and 1 mM TCEP as loading buffer and the
148 same buffer containing 1 M NaCl was used for elution. The final buffer after
149 AEC was 20 mM HEPES pH 7.5, 250 mM NaCl, and 1 mM TCEP. The
150 proteins were concentrated to at least 5 mg/ml based on their calculated
151 extinction coefficient using ProtParam (SwissProt) and then flash frozen for
152 storage at -80°C.

153

154 *ATPase assay*

155 dsDNA substrates used:

156 F26,50 contains a fluorescein moiety covalently attached to thymine (*);

157 5`GACTACGTACTGTTACGGCTCCATCT*CTACCGCAATCAGGCCAGA
158 TCTGC 3`

159 The reverse complementary sequence to F26,50;

160 5`GCAGATCTGGCCTGATTGCGGTAGCGATGGAGCCGTAACAGTACG
161 TAGTC 3`

162 F26,50 without the fluorescein moiety;

163 5`GACTACGTACTGTTACGGCTCCATCTCTACCGCAATCAGGCCAGAT
164 CTGC 3`

165 The NADH-coupled ATPase assay was performed as described previously ²² in
166 plate reader format. Imaging buffer containing the NADH-reaction components
167 was supplemented with 1 mM fresh TCEP, protein (100 nM (equimolar
168 concentrations for XPD N-p44 and XPD p44/p62)), and 50 nM of DNA
169 substrate. The reaction was started with the addition of 1 mM ATP to each well,
170 and the change in OD340 (NADH) was monitored every 8 seconds/well over 30

171 minutes at room temperature in a Clariostar plate reader. The rates of NADH
172 consumption were used to calculate k_{cat} . Reactions were repeated 3 times, and
173 S.E.M used as errors values.

174

175 *In vitro helicase assay*

176 Helicase activity was analyzed utilizing a fluorescence-based helicase assay.

177 We used an open fork substrate with a Cy3 label at the 3' end of the

178 translocated strand where unwinding of the DNA substrate reduces quenching
179 of the Cy3 fluorescence.

180 5' AGCTACCATGCCTGCACGAATTAAGCAATTCGTAATCATGGTCATA

181 GC-Cy3 3' and a dabcy1 modification on the 5' end of the opposite strand

182 5' Dabcy1-

183 GCTATGACCATGATTACGAATTGCTTGGAATCCTGACGAACTGTAG

184 3'

185 Assays were carried out in 20 mM HEPES pH 7.5, 50 mM KCl, 5 mM MgCl₂,

186 and 1 mM TCEP. DNA was used at a concentration of 250 nM. Helicase

187 activity was measured with equimolar concentrations of XPD, p44, and/or p62.

188 The mix of reagents, with the exception of ATP, were preincubated at 37°C and

189 the reaction was subsequently started with the addition of 5 mM ATP. Kinetics

190 were recorded with a Flourostar Optima plate reader (BMG labtech).

191 Fluorescence was detected at an excitation wavelength of 550 nm (slit width, 2

192 nm) and an emission wavelength of 570 nm (slit width, 2 nm). Initial velocities

193 were fitted with the MARS software package (BMG labtech) and represent the

194 averages of at least three different reactions and two independent protein

195 batches.

196

197 *Single Molecule DNA Tightrope Assay*

198 For a detailed protocol see ¹⁸. p44/p62 interactions with DNA were studied in

199 imaging buffer (20 mM Tris pH 8.0, 10 mM KCl (100 mM for high salt), 5 mM

200 MgCl₂, 1 mM TCEP). Videos for diffusion analysis were collected between 30
201 seconds and 5 minutes at 10 frames per second. Video analysis was performed
202 in ImageJ as described previously¹⁷.

203

204 **Acknowledgements**

205 We would like to thank the members of the Kad group for useful discussions.
206 This work was supported by the Biotechnology and Biological Sciences
207 Research Council BB/P00847X/1, BB/M019144/1, BB/I003460/1 to NMK and
208 BB/M01603X/1 to JTB and by the German Research Foundation KI-562/7-1 to
209 CK. The authors declare no conflict of interest.

210

211 **Author contributions**

212 Collected data: JTB, JK, WK. Designed experiments: JTB, JK, CK, NMK.

213 Analysed Data: JTB, JK, NMK. Wrote paper: JTB, JK, CK, NMK.

214

215 **References**

216

- 217 1 Compe, E. & Egly, J. M. TFIIH: when transcription met DNA repair. *Nat*
218 *Rev Mol Cell Biol* **13**, 343-354, doi:10.1038/nrm3350 (2012).
- 219 2 Roy, R. *et al.* The DNA-dependent ATPase activity associated with the
220 class II basic transcription factor BTF2/TFIIH. *J Biol Chem* **269**, 9826-
221 9832 (1994).
- 222 3 Luo, J. *et al.* Architecture of the Human and Yeast General Transcription
223 and DNA Repair Factor TFIIH. *Mol Cell* **59**, 794-806,
224 doi:10.1016/j.molcel.2015.07.016 (2015).
- 225 4 Araujo, S. J. *et al.* Nucleotide excision repair of DNA with recombinant
226 human proteins: definition of the minimal set of factors, active forms of
227 TFIIH, and modulation by CAK. *Genes Dev* **14**, 349-359 (2000).
- 228 5 Svejstrup, J. Q. *et al.* Different forms of TFIIH for transcription and DNA
229 repair: holo-TFIIH and a nucleotide excision repairsome. *Cell* **80**, 21-28
230 (1995).
- 231 6 Sung, P. *et al.* Human xeroderma pigmentosum group D gene encodes a
232 DNA helicase. *Nature* **365**, 852-855, doi:10.1038/365852a0 (1993).

- 233 7 Coin, F. *et al.* Mutations in the XPD helicase gene result in XP and TTD
234 phenotypes, preventing interaction between XPD and the p44 subunit of
235 TFIIH. *Nature Genetics* **20**, 184-188, doi:Doi 10.1038/2491 (1998).
- 236 8 Kuper, J. *et al.* In TFIIH, XPD helicase is exclusively devoted to DNA
237 repair. *PLoS biology* **12**, e1001954 (2014).
- 238 9 Coin, F., Oksenysh, V. & Egly, J. M. Distinct roles for the XPB/p52 and
239 XPD/p44 subcomplexes of TFIIH in damaged DNA opening during
240 nucleotide excision repair. *Mol Cell* **26**, 245-256,
241 doi:10.1016/j.molcel.2007.03.009 (2007).
- 242 10 Liu, H. *et al.* Structure of the DNA repair helicase XPD. *Cell* **133**, 801-
243 812, doi:10.1016/j.cell.2008.04.029 (2008).
- 244 11 Greber, B. J., Toso, D. B., Fang, J. & Nogales, E. The complete structure
245 of the human TFIIH core complex. *Elife* **8**, doi:10.7554/eLife.44771
246 (2019).
- 247 12 Bernardes de Jesus, B. M., Bjoras, M., Coin, F. & Egly, J. M. Dissection
248 of the molecular defects caused by pathogenic mutations in the DNA
249 repair factor XPC. *Mol Cell Biol* **28**, 7225-7235,
250 doi:10.1128/MCB.00781-08 (2008).
- 251 13 Buechner, C. N. *et al.* Strand-specific recognition of DNA damages by
252 XPD provides insights into nucleotide excision repair substrate
253 versatility. *J Biol Chem* **289**, 3613-3624, doi:10.1074/jbc.M113.523001
254 (2014).
- 255 14 Gervais, V. *et al.* TFIIH contains a PH domain involved in DNA
256 nucleotide excision repair. *Nat Struct Mol Biol* **11**, 616-622,
257 doi:10.1038/nsmb782 (2004).
- 258 15 Gileadi, O., Feaver, W. J. & Kornberg, R. D. Cloning of a subunit of
259 yeast RNA polymerase II transcription factor b and CTD kinase. *Science*
260 **257**, 1389 (1992).
- 261 16 Matsui, P., DePaulo, J. & Buratowski, S. An interaction between the Tfb1
262 and Ssl1 subunits of yeast TFIIH correlates with DNA repair activity.
263 *Nucleic Acids Research* **23**, 767-772 (1995).
- 264 17 Kad, N. M., Wang, H., Kennedy, G. G., Warshaw, D. M. & Van Houten,
265 B. Collaborative dynamic DNA scanning by nucleotide excision repair
266 proteins investigated by single- molecule imaging of quantum-dot-labeled
267 proteins. *Mol Cell* **37**, 702-713, doi:10.1016/j.molcel.2010.02.003 (2010).
- 268 18 Springall, L., Inchingolo, A. V. & Kad, N. M. DNA-Protein Interactions
269 Studied Directly Using Single Molecule Fluorescence Imaging of
270 Quantum Dot Tagged Proteins Moving on DNA Tightropes. *Methods*
271 *Mol Biol* **1431**, 141-150, doi:10.1007/978-1-4939-3631-1_11 (2016).
- 272 19 von Hippel, P. H. & Berg, O. G. Facilitated target location in biological
273 systems. *J Biol Chem* **264**, 675-678 (1989).

- 274 20 Schurr, J. M. The one-dimensional diffusion coefficient of proteins
275 absorbed on DNA. *Biophysical Chemistry* **9**, 413-414, doi:10.1016/0301-
276 4622(75)80057-3 (1979).
- 277 21 Kuper, J. *et al.* In TFIIF, XPD Helicase Is Exclusively Devoted to DNA
278 Repair. *Plos Biology* **12**, doi:ARTN e1001954
279 10.1371/journal.pbio.1001954 (2014).
- 280 22 Barnett, J. T. & Kad, N. M. Understanding the coupling between DNA
281 damage detection and UvrA's ATPase using bulk and single molecule
282 kinetics. *FASEB journal* **33**, 763-769, doi:10.1096/fj.201800899R (2019).
283
284